

Central Lancashire Online Knowledge (CLoK)

Title	Inhibition of corrosion causing <i>Pseudomonas aeruginosa</i> using plasma activated water
Type	Article
URL	https://clock.uclan.ac.uk/id/eprint/39991/
DOI	https://doi.org/10.1111/jam.15391
Date	2022
Citation	Asimakopoulou, Eleni, Ekonomou, Sotirios, Papakonstantinou, Pagona, Doran, Olena and Stratakis, Alexandros (2022) Inhibition of corrosion causing <i>Pseudomonas aeruginosa</i> using plasma activated water. <i>Journal Of Applied Microbiology</i> , 132 (4). pp. 2781-2794. ISSN 1364-5072
Creators	Asimakopoulou, Eleni, Ekonomou, Sotirios, Papakonstantinou, Pagona, Doran, Olena and Stratakis, Alexandros

It is advisable to refer to the publisher's version if you intend to cite from the work.
<https://doi.org/10.1111/jam.15391>

For information about Research at UCLan please go to <http://www.uclan.ac.uk/research/>

All outputs in CLoK are protected by Intellectual Property Rights law, including Copyright law. Copyright, IPR and Moral Rights for the works on this site are retained by the individual authors and/or other copyright owners. Terms and conditions for use of this material are defined in the <http://clock.uclan.ac.uk/policies/>

1 **Inhibition of corrosion causing *Pseudomonas aeruginosa* using plasma activated water**

2

3 Eleni Asimakopoulou^{1,*}, Sotirios I. Ekonomou², Pagona Papakonstantinou³, Olena Doran⁴,
4 Alexandros Ch. Stratakos^{5,*}

5

6 ¹ School of Engineering, University of Central Lancashire, Flyde Rd, Preston, PR1 2HE,
7 United Kingdom, (<https://orcid.org/0000-0001-5644-1372>), Easimakopoulou@uclan.ac.uk

8 ² Centre for Research in Biosciences, Faculty of Health and Applied Sciences (HAS),
9 University of the West of England, Coldharbour Ln, Bristol, BS16 1QY, United Kingdom
10 (<https://orcid.org/0000-0003-3010-3038>), Sotirios.Oikonomou@uwe.ac.uk

11 ³ Engineering Research Institute, School of Engineering, Ulster University, Newtownabbey
12 BT37 0QB, United Kingdom, (<https://orcid.org/0000-0003-0019-3247>),
13 p.papakonstantinou@ulster.ac.uk

14 ⁴ Faculty of Health and Applied Sciences (HAS), University of the West of England,
15 Coldharbour Ln, Bristol, BS16 1QY, United Kingdom (<https://orcid.org/0000-0002-6391-3988>), Olena.Doran@uwe.ac.uk

17 ⁵ Centre for Research in Biosciences, Faculty of Health and Applied Sciences (HAS),
18 University of the West of England, Coldharbour Ln, Bristol, BS16 1QY, United Kingdom,
19 (<https://orcid.org/0000-0001-6117-7385>), Alexandros.Stratakos@uwe.ac.uk

20 * Corresponding authors info:

21 Dr Eleni Asimakopoulou, email: easimakopoulou@uclan.ac.uk, telephone number: (0044)
22 01772 894222

23 Dr Alexandros Stratakos, email: alexandros.stratakos@uwe.ac.uk, telephone number: (0044)
24 01173284743

25

26 **Running headline:** Plasma activated water against microbial corrosion

27 **Abstract**

28 **Aims:** The cost of Microbiologically Influenced Corrosion (MIC) significantly affects a wide
29 range of sectors. This study aims to assess the efficiency of a novel technology based on the
30 use of plasma activated water (PAW) in inhibiting corrosion caused by bacteria.

31 **Methods and Results:** This study evaluated the effectiveness of PAW, produced by a plasma
32 bubble reactor, in reducing corrosion causing *Pseudomonas aeruginosa* planktonic cells in tap
33 water and biofilms grown onto stainless steel (SS) coupons. Planktonic cells and biofilms were
34 treated with PAW at different discharge frequencies (500-1500 Hz) and exposure times (0-20
35 min). *P. aeruginosa* cells in tap water were significantly reduced after treatment, with higher
36 exposure times and discharge frequencies achieving higher reductions. Also, PAW treatment
37 led to a gradual reduction for young and mature biofilms, achieving >4-Log reductions after
38 20 min. Results were also used to develop two predictive inactivation models.

39 **Conclusions:** This work presents evidence that PAW can be used to inactivate both planktonic
40 cells and biofilms of *P. aeruginosa*. Experimental and theoretical results also demonstrate that
41 reduction is dependent on discharge frequency and exposure time.

42 **Significance and Impact of the Study:** This work demonstrates the potential of using PAW
43 as means to control MIC.

44

45 **KEYWORDS:** plasma activated water, biofilm, intracellular ATP levels, microbial corrosion,
46 *P. aeruginosa*.

47

48 INTRODUCTION

49 Metal corrosion can be significantly accelerated by the presence and activity of
50 microorganisms, a process that is also known as biocorrosion or Microbiologically Influenced
51 Corrosion (MIC) (Phan et al. 2021) and is responsible for 20% of metal corrosion damages
52 (Flemming, 1996). The cost of corrosion in industrialised countries was estimated to be 3.4%
53 of the global GDP in 2013, and if corrosion protection and design were properly applied, a 15-
54 35% loss reduction could be achieved (Koch et al. 2016). Its direct costs affect a wide range of
55 sectors, including agriculture, forestry and fishing, mining, manufacturing (e.g., chemical
56 processing, nuclear, oil, gas, underground pipeline, water treatment, food production, highway
57 maintenance, aviation, metal working, marine, shipping and fire protection), electricity supply,
58 water supply, waste management, accommodation, and food service activities, transportation,
59 and storage. Indirect costs are associated with environmental, regulatory, and human costs,
60 making cost estimation even more challenging (Little et al. 2020).

61 Until recently, corrosion research was primarily focused on operational aspects such as the
62 assessment of the corrosion damage and mineral deposits impact on the functionality of
63 systems, mechanical operations of equipment and unanticipated failures (Bardal, 2004). Those
64 are more frequently encountered in systems comprised of widely used, cost-effective, but less
65 resistant groups of metal alloys such as carbon steels (Herrera and Videla, 2009) and stainless
66 steels (Cheng et al. 2009). The extent of those damages and mineral deposits is influenced by
67 both materials and the environment (Lyon, 2014).

68 Lately, more fundamental research was conducted aiming to investigate MIC associated
69 phenomena and advised to approach the subject systematically by monitoring the microbial
70 activity of single bacteria (Kermani and Harrop, 2019). Different types of aerobic and
71 anaerobic bacteria are associated with MIC; among them, the most commonly met are the acid-
72 producing, sulphur reducing and iron related bacteria (Su and Fuller, 2014) as well as others,

73 such as *Pseudomonas aeruginosa* (Li et al. 2016; Jia et al. 2017). *P. aeruginosa* MIC
74 mechanism and associated bacteria-metal reactions have been extensively investigated, and its
75 presence is proven to accelerate corrosion (Abdolahi et al. 2014). There are several studies that
76 confirm its involvement in the corrosion process of different types of metals e.g., mild steel
77 (Xu et al. 2017), stainless steel (Xu et al. 2016; Jia et al. 2017; Xu et al. 2017) and aluminium
78 (Xu et al. 2017).

79 Research in MIC is spanning four main areas: diagnose, monitor, modelling and prevention.
80 To achieve the latter, numerous treatments are customarily used, and the most common ones
81 include sanitation, physical, chemical treatment, biological methods, use of coatings and
82 cathodic protection (Enning and Garrelfs, 2014; Ibrahim et al. 2018; Little et al. 2020). The
83 solution of applying coating specifically designed for each application appears to be promising,
84 however this is not always feasible and practical. An efficient way to limit microbial growth is
85 through physical treatment (e.g. pigging, ultraviolet irradiation, ultrasonic, chemical and
86 biological treatments) of natural or industrial water aiming to inhibit the microorganisms
87 responsible for causing corrosion (Little et al. 2020). Recent studies have revealed that indirect
88 application of Cold Atmospheric Plasma (CAP) at ambient air conditions can significantly
89 decrease the microbial load (Pasquali et al. 2016; Katsigiannis et al. 2021). Also, in recent
90 years, a new mode of CAP, i.e., Plasma-activated Water (PAW) activities has drawn attention
91 (Julák et al. 2012; Chen et al. 2018) as it can be applied to inhibit/kill microorganisms in
92 surfaces and systems in an environmentally friendly, cost-effective, and practical way. Lately,
93 the application of PAW has been investigated (Tan and Karwe, 2021) and has been proven an
94 effective technique for inactivating inner-pipe surfaces formed biofilms, also recognised as a
95 novel technology with significantly decreased environmental cost (Zhou et al. 2020).
96 Despite a large number of recent publications related to MIC, an effective and practical
97 technological solution to tackle MIC related problems is yet to be found (Little et al. 2020). To

98 meet this challenge, the current experimental work aims to assess the efficiency and
99 antimicrobial mechanism of PAW against corrosion causing *P. aeruginosa* as well as identify
100 optimal operational conditions for PAW treatment.

101 **MATERIALS AND METHODS**

102 **Bacterial cultivation**

103 Experiments were conducted using PAO1, a *P. aeruginosa* strain. The *P. aeruginosa* culture
104 was prepared in Luria-Bertani (LB) liquid medium enriched with KNO₃ (LB-NO₃). The media
105 formulation of the agar medium LB-NO₃ included 10 g tryptone, 10 g KNO₃ 5 g yeast extract,
106 and 5 g NaCl per litre of deionised water. KNO₃ was added to the LB medium to support
107 anoxic growth of *P. aeruginosa* PAO1 (Line et al. 2014). The pH was adjusted to 7.0 by
108 applying a solution of NaOH. To mitigate any possible O₂ entry, L-cysteine at a concentration
109 of one hundred ppm (w/w), was added to the culture medium as O₂ scavenger. The L-cysteine
110 solution was filter-sterilised using MF-MilliporeTM membrane filter of a pore size of 0.22 µm
111 (Merck KGaA, Darmstadt, Germany) before it was added to the medium. Dissolved oxygen
112 was removed from all liquid solutions by flushing them with filter sterilised N₂ in order to
113 maintain anoxic growth of *P. aeruginosa*. 304 Stainless Steel (SS) sheet were used to cut the
114 rectangular shaped coupons (1 cm x 1 cm) used in this work. Coupons were sterilised in 75%
115 ethanol solution for 2 h, dried and exposed to UV light for 30 min prior to use. A N₂ chamber
116 was used for anaerobic manipulations. The biofilms were grown in anaerobic vials, following
117 the procedure described by Jia et al. (2017). One hundred ml of LB-NO₃ medium, with and
118 without the addition of the *P. aeruginosa* culture, was added to each anaerobic vial. The
119 experiments were conducted on three replicate coupons. The initial bacterial concentration
120 after inoculation with *P. aeruginosa* was approximately 10⁴⁻⁵ Log CFU ml⁻¹. The vials were
121 closed and incubated at 37°C for 2, 5, or 7 days. After the incubation, the coupons were
122 removed, and PAW treated under different conditions as described below. Before PAW

123 treatment, the coupons were gently rinsed with sterile phosphate-buffered saline to remove the
124 non-adhered and loosely attached bacterial cells.

125 **Plasma bubble reactor**

126 A schematic representation of the plasma bubble reactor (PBR) used to generate the PAW is
127 illustrated in Figure 1. The PBR consisted of an acrylic tube with a 140 mm length that
128 constituted of machined caps at each end. Those caps had 4 mm stainless-steel rod positioned
129 coaxially at the interior of the full length of the tube, acting as high voltage electrodes. A 5 mm
130 wide strip of adhesive copper tape was positioned at the exterior of the ground electrode and
131 was connected to the ground wire of the plasma power supply. Plasma was generated under
132 atmospheric conditions, and the electrical discharges were provided by a high voltage power
133 supply (PlasmaLeap Technologies, Ireland) specifically designed to supply a wide range of
134 voltages at discharge frequencies.

135 The acrylic tube of the PBR, submerged into the water, was perforated with ten 2 mm holes
136 located 8 mm from its base. Compressed air to the PBR was supplied at a flow rate of 1 l min⁻¹
137 via a tube placed at the opposing end of the acrylic tube. The electrically discharged bubbles
138 leaving the reactor, through the holes entered the water, and subsequently, the generated
139 reactive species at their interior, contacted the water via their bubble surface-water interface.

140 **PAW treatment of stainless-steel (SS) coupons and biofilm enumeration**

141 The plasma reactor was filled with 100 ml of sterile tap water. Control SS coupons (no PAW
142 treatment) were immersed in water and placed on the bottom of the reactor, with just the airflow
143 on, for 15 min without igniting the plasma. For treated samples, coupons were placed in the
144 reactor and subsequently the PBR was turned on. The reactor was allowed to run for different
145 times (5, 10, 15, and 20 min), at 150 V (voltage applied at the high voltage transformer), 100-
146 μ s duty cycle (time during which the energy from the power supply unit is transferred to HV
147 transformer resonance circuit) and 60 kHz resonance frequency (resonance frequency of

148 resonance circuit). Three different discharge frequencies were investigated (500, 1000, and
149 1500 Hz).

150 SS coupons with adhered biofilm cells of different maturity were treated directly in PBR for 0,
151 5, 10, 15, and 20 min. After treatment, the SS coupons were positioned in a sterile container
152 with 10 mL maximum recovery diluent (MRD) (Oxoid, UK) and 1 g glass beads caliber of 0.1
153 mm diameter. To detach the surviving biofilm cells from the SS coupons, samples were
154 vortexed for 60 s. Subsequently, 10-fold dilutions were prepared in MRD to enumerate the
155 surviving biofilm cells. An aliquot of 100- μ l was used from the appropriate 10-fold serial
156 dilutions and was spread plated on Tryptone Soya Agar (TSA, Oxoid, UK). Plates were
157 incubated at 37 °C for 24 h and the biofilm cells expressed as Log CFU cm⁻².

158 **PAW treatment and enumeration of *P. aeruginosa***

159 *P. aeruginosa* can exist in the water before it attaches to surfaces and begin to form biofilms
160 and subsequently influence the physicochemical metal-environment interactions, thus
161 enhancing MIC (Li et al. 2016; Jia et al. 2017). To investigate if PAW can inactivate this
162 microorganisms in its planktonic form, 100- μ l of the *P. aeruginosa* (prepared as described
163 above) was inoculated into 100 ml of tap water. After inoculation, the bacterial concentration
164 was approximately 10⁵ Log CFU ml⁻¹. Control samples received no treatment (0 min; only
165 airflow was on for 15 min without igniting the plasma). For the rest of the PAW treatments,
166 the PBR was turned on and allowed to run for different time periods (0, 5, and 10 min) at 150
167 V, 100- μ s duty cycle, 60 kHz resonance frequency and 500, 1000, and 1500 Hz discharge
168 frequencies. The planktonic cells were treated inside the reactor. Immediately after treatment,
169 an aliquot (1 ml) of the treated tap water was added to 9 ml of MRD and subsequently, further
170 suitable 10-fold dilutions were prepared. An aliquot of 100- μ l was used from the appropriate
171 10-fold serial dilutions and was spread plated on Trypticase Soy Agar (TSA, Oxoid, UK).

172 Plates were incubated at 37 °C for 24 h, and planktonic *P. aeruginosa* cells were expressed as
173 Log CFU ml⁻¹.

174 **Physicochemical properties of PAW**

175 PAW was generated at a discharge frequency of 1500 Hz for 15 minutes, and the measurements
176 of pH, electrical conductivity (EC), H₂O₂, NO₂⁻, and NO₃⁻ concentrations were taken
177 immediately after treatment. Values of EC and pH were measured using an electronic
178 conductivity meter (Jenway 4200, UK) and a pH meter (FiveEasy, Mettler Toledo, UK),
179 respectively. H₂O₂ concentration was determined using the titanium oxysulphate (TiOSO₄;
180 Sigma-Aldrich) method. According to that method, TiOSO₄ reacts with H₂O₂, and produces a
181 yellow-coloured complex (pertitanic acid). Subsequently, the H₂O₂ concentration was
182 determined spectrophotometrically (Mai-Prochnow et al. 2021b). Nitrite concentration was
183 determined by using the Griess assay, a chemical reaction that uses N-(1-naphthyl)-ethylene
184 diamine hydrochloride under sulfanilic acidic conditions, resulting in the formation of a
185 magenta-coloured azo dye. Nitrate (NO₃⁻) concentration was determined using a nitrate assay
186 kit (Sigma, UK) that is based on its reaction with 2, 6-dimethylphenol (DMP). To eliminate
187 nitrite interference, all PAW samples were pre-treated using sulfamic acid (Zhao et al. 2020)
188 prior to analysis.

189 Individual standard curves of known H₂O₂, NaNO₂ and NaNO₃ concentration were prepared to
190 convert the absorbance to H₂O₂, NO₂⁻, NO₃⁻, concentrations.

191 **Membrane integrity**

192 Protein leakage was used to assess membrane integrity of *P. aeruginosa* suspension cells after
193 PAW treatment at 500, 1000, and 1500 Hz discharge frequencies. This was achieved by
194 measuring protein concentration in the supernatants using a Pierce BCA protein kit
195 (ThermoScientific, U.K.) (Sadiq et al. 2017) and using untreated samples as controls.

196 **Intracellular adenosine triphosphate levels**

197 The effect of PAW treatment on the intracellular adenosine triphosphate (ATP) levels was
198 determined using the procedure described by Stratakos et al. (2018). The 24 hours old *P.*
199 *aeruginosa* cultures were centrifuged at 5000 x g for 5 min. The produced pellets were washed
200 three times using phosphate-buffered saline, and centrifugation was used to collect the cells.
201 The pellets were re-suspended in one millilitre of PAW production at PBR discharge
202 frequencies of 500, 1000, or 1500 Hz respectively for 15 min. Subsequently, all samples were
203 stored for 15 min at 37°C. Cells were centrifuged at 5000 x g for 5 min and treated with a lysis
204 buffer (Roche, U.K.) for another 5 min at room temperature to extract the intracellular ATP.
205 The intracellular ATP quantity was determined with the ATP assay kit (ATP bioluminescence
206 assay kit HS II, Roche, U.K.); 100 µl of ATP luciferase reagent were added to the 100 µl of
207 supernatant in solid white 96-well plates. Then to determine ATP concentrations a microplate
208 reader (FLUOstar Omega, BMG Labtech, U.K.) was used using untreated samples as controls.

209 **Statistical analysis and modelling**

210 All treatments were performed three times, and each sample was analyzed twice and averaged
211 before statistical analysis. Statistical analysis was done with Excel Microsoft® Office 365 (ver.
212 16.48). Tukey post hoc tests were used to compare sample data using the IBM® SPSS®
213 statistics 26 software for macOS (SPSS Inc., US). A 5.0 % level of significance, *P*, was used,
214 and thus results were considered statistically significant when *P* was less than 0.05 ($P < 0.05$).
215 The fitting procedure for modelling of inactivation kinetics was performed using GInaFiT
216 software (Geeraerd et al. 2005).

217 **RESULTS**

218 **The efficacy of PAW treatment against planktonic cells of *P. aeruginosa***

219 The effect of PAW treatment on planktonic *P. aeruginosa* cells after 5, 10, and 15 min exposure
220 to different PBR discharge frequencies (500, 1000, and 1500 Hz) is presented in Figure 2. The

221 initial population of *P. aeruginosa* control cells without plasma treatment in tap water was 4.99
222 Log CFU ml⁻¹.

223 The population of *P. aeruginosa* in tap water was significantly reduced after 5 min of PAW
224 treatment and reached 0.44, 1.77, and 2.51 Log CFU ml⁻¹ at 500, 1000 and 1500 Hz, PBR
225 discharge frequencies respectively (Fig 2, $P < 0.05$). *P. aeruginosa* cells, treated with PAW for
226 10 min resulted in a significant reduction of the cell numbers by 1.26 and 2.88 Log CFU ml⁻¹
227 at 500 and 1000 Hz, respectively (Fig 2, $P < 0.05$). However, PAW treatment at 1500 Hz
228 resulted in a reduction below the detection limit (>3.99 Log CFU ml⁻¹) (Fig 2). After 15 min
229 of PAW treatment at 1000 and 1500 Hz, the bacterial numbers of *P. aeruginosa* were reduced
230 below the detection limit, while PAW treatment at 500 Hz resulted in a significant reduction,
231 of 1.69 Log CFU ml⁻¹ (Fig 2, $P < 0.05$).

232 The reduction of *P. aeruginosa* planktonic cells under the investigated discharge frequencies
233 of PAW treatment depended on the exposure time. As shown in Fig 2, all the PAW treatments
234 resulted in a significant decrease in the number of the planktonic cells after 5- and 10-min
235 exposure (Fig 2, $P < 0.05$). In the case of *P. aeruginosa* cells treated at 500 Hz, significant
236 bacterial reduction was observed for all the exposure times investigated. There were no
237 significant differences between the effect of plasma treatments at 1000 and 1500 Hz (neither
238 at 10 nor 15 min) when bacterial numbers were reduced close to or below the detection limit
239 (Fig 2, $P > 0.05$).

240 **The efficacy of PAW treatment against biofilms of *P. aeruginosa***

241 *P. aeruginosa* can form biofilms on the surface of stainless-steel pipes, accelerating MIC (Jia
242 et al. 2017). This study investigated whether PAW treatment can be applied to reduce the more
243 resistant *P. aeruginosa* biofilms. To assess the efficacy of PAW treatment, further experiments
244 were carried out using the most effective PBR discharge frequency of 1500 Hz against the
245 biofilms of *P. aeruginosa* grown on stainless-steel coupons for 24, 48, and 72 h. Reduction

246 levels of *P. aeruginosa* biofilms are presented in Figure 3. Plasma discharge in bubbles for 5
247 min reduced the 24, 48, and 72 h attached biofilm cells of *P. aeruginosa* by 2.77, 2.20, and
248 1.42 Log CFU cm²⁻¹, respectively (Fig 3, *P* < 0.05). The same trend was observed after 10 min
249 of PAW treatment with increased efficacy, where bacterial numbers for biofilms grown for 24,
250 48, and 72 h were reduced significantly by 3.77, 3.12, and 2.55 Log CFU cm²⁻¹, respectively
251 (Fig 3, *P* < 0.05). After 15 min of exposure, the 24 h old biofilms were reduced by >4.00 Log
252 CFU cm⁻², below the detection limit of 2.00 Log CFU cm⁻² (Fig 3). However, *P. aeruginosa*
253 48 and 72 h mature biofilms decreased below the detection limit (2.00 Log CFU cm²⁻¹) after
254 20 min of exposure at PAW treatment, corresponding to >4.15 and >4.24 log reduction of
255 CFUcm⁻² (Fig 3).

256 There was a significant reduction in bacteria population for the 24 h biofilms, exposed for 5
257 and 10 min (Fig 3, *P* < 0.05). In addition, *P. aeruginosa* 48 and 72 h mature biofilms showed
258 significant differences in reductions achieved at all the PAW exposure times (Fig 3, *P* < 0.05).

259 **Physicochemical properties of PAW treatment**

260 The PBR that was used to generate PAW at 1500 Hz discharge frequency and 15 min of
261 exposure time produced different reactive species. The physicochemical properties of PAW
262 treatment are shown in Table 1. The initial pH value of the tap water was 7.56±0.024, which
263 decreased to 5.94±0.038 after 15 min exposure (*P* < 0.05). Also, the EC value of the water
264 significantly increased (*P* < 0.05), which suggests the formation of reactive molecular species
265 under these conditions. The specific reactive species, produced as the result of complex
266 chemical reactions between the plasma and liquid (tap water), that were detected and quantified
267 were H₂O₂ (0.028±0.002 mg ml⁻¹), NO²⁻ (0.037± 0.001 mg ml⁻¹), and NO³⁻ (0.039± 0.001 mg
268 ml⁻¹).

269 **Effect of PAW treatment on *P. aeruginosa* protein release**

270 Data in Figure 4 show the amount of protein released from *P. aeruginosa* planktonic cells
271 treated with PAW at 500, 1000, and 1500 Hz of PBR discharge frequency. Protein leakage
272 from PAW-treated *P. aeruginosa* cells at 1000 and 1500 Hz significantly increased compared
273 to that from untreated cells (control) and from the cells treated at 500 Hz (Fig 4, $P < 0.05$). The
274 highest release of proteins for the PAW-treated *P. aeruginosa* planktonic cells was observed at
275 1000 and 1500 Hz, respectively. The data suggest that there was a gradual increase in protein
276 release in the cell suspension with increase in discharge frequency.

277 **Effect of PAW treatment on *P. aeruginosa* intracellular ATP levels**

278 Results on the effect of PAW treatment on *P. aeruginosa* Intracellular ATP levels at different
279 discharge frequencies are presented in Figure 5. The ATP calibration curve showed a positive
280 linear relationship between relative luminescence units and ATP level, which can be described
281 by the following equation: $y = 475926x + 22826$; $R^2 = 0.986$. The level of intracellular ATP
282 of *P. aeruginosa* decreased significantly as the discharge level of PAW treatment increased
283 from 500 to 1000 and 1500 Hz (Fig 5, $P < 0.05$). The initial ATP concentration of the untreated
284 (Control) *P. aeruginosa* cells was 0.340 mM, while after PAW treatment at 500, 1000, and
285 1500 Hz, it was reduced to 0.164, 0.073, and 0.042 mM, respectively ($P < 0.05$).

286 **Modelling of inactivation kinetics**

287 The responses of the different parameters in the microbial population of *P. aeruginosa* to
288 different exposure times were fitted using a log-linear regression model (Bigelow and Etsy,
289 1920). Analysis of the experimental dataset of the microbial population of *P. aeruginosa* was
290 performed using a weighted least square linear fit model. The Coefficient of Determination
291 (COD), also known as R^2 , was used as a statistical measure to assess the quality of each linear
292 regression fit. The linear regression model, Equation (1), was used to estimate the kinetic
293 inactivation parameter, D_T , for the different PBR discharge frequencies for the planktonic *P.*

294 *aeruginosa* cells and the young, 24 h old, and mature, 48 and 72 h old, biofilms. In the Equation
295 (1), N represents the microbial population at time t , and N_o is the experimentally determined
296 initial microbial population. Microbial population measurements below the level of detection
297 (D) were handled using a substitution method (Ogden, 2010). According to the substitution
298 method every result below D , also known as censored data, is substituted with an estimate, for
299 what it might be. Traditional options for handling censored data include discarding non-detect
300 data and using simple substitution methods (treating non-detects as zero, half the detection
301 limit, at the detection limit, or the detection limit/ $\sqrt{2}$) (Levine et al. 2009; EPA, 2006). Instead
302 of eliminating censored data from the data set, setting them as zero or D values, that has been
303 proved to yield erroneous results (Silvestri et al. 2017), in the current study values bellow D ,
304 were substituted with $D/2$ (Levine, 2006; Ogden, 2010).

305 Tables 2 and 3 present the model parameters and their measures of statistical dispersion namely
306 the standard error (SE), mean sum of R^2 , root mean sum of R^2 , R^2 and adjusted R^2 for biofilms
307 of different maturity and PBR discharge frequencies. Figure 6 shows the relevant fitted
308 inactivation curves for biofilms of *P. aeruginosa* grown for 24, 48, and 72 h and treated with
309 PAW at a discharge frequency of 1500 Hz. The developed model can be reliably used to
310 describe the inactivation curves. Good statistical fit was observed for biofilms of different
311 maturity with estimated adjusted R^2 values ranging from 0.9005 to 0.9445. The calculated
312 values for the inactivation parameter D_T for each biofilm ranged from 3.11 for the 24 h old
313 biofilms to 4.34 for the 48 h old biofilms. The relevant model parameters and associated errors
314 for *P. aeruginosa* planktonic cells after PAW treatment at different PBR discharge frequencies
315 are presented in Table 3. Figure 7 shows the inactivation curves for the different exposure
316 times. The inactivation parameter D_T tends to decrease with the increase of PBR discharge
317 frequencies, with the values ranging from 8.53 at 500 Hz to 2.24 at 1500 Hz. The accuracy of

318 the developed model is supported by the statistical parameters and evaluation of the fitting
319 curves (Fig 7).

$$320 \quad \log N = \log N_o - \frac{t}{D_T} \quad (1)$$

321 **DISCUSSION**

322 MIC is a destructive phenomenon that affects stainless-steel surfaces, which are widely used
323 by a range of industries, including the companies producing material for various equipment or
324 building purposes. This study proposes an innovative approach to tackle the issue of MIC.
325 The approach is based on the application of PAW against *P. aeruginosa*, which is known to
326 cause corrosion on stainless-steel surfaces (Gabriel et al. 2016). Although, corrosion inhibition
327 itself from *P. aeruginosa* was not assessed, this work presents the first evidence that PAW is
328 effective in inactivating both planktonic cells and biofilms of *P. aeruginosa* grown under
329 anaerobic conditions. Furthermore, the results of this study were rationalized by means of two
330 predictive inactivation models.

331 During the last decade, cold plasma treatment has been attracting attention as a green
332 technology for the inactivation of spoilage and pathogenic bacteria on different matrices
333 (Ehlbeck et al. 2010; Pasquali et al. 2016; Jayathunge et al. 2019; Ekonomou and Boziaris,
334 2021), as well as a method for decontamination of industrial surfaces and medical equipment
335 (Ben Belgacem et al. 2017; Alshraiedeh et al. 2020; Gonzalez-Gonzalez et al. 2021). Recently,
336 the development of PAW offered a new opportunity as a promising decontamination method
337 for the preservation of food (Ma et al. 2015; Liao et al. 2018; Thirumdas et al. 2018) and wound
338 healing in the medical industry (Chen et al. 2017; Kaushik et a., 2017), and as an alternative
339 disinfectant for the inactivation of bacteria in water (Pan et al. 2017; Zhou et al. 2018). In this
340 work, PAW showed a high antimicrobial effect against planktonic cells of *P. aeruginosa*. The
341 efficacy of the treatment increased by extending the cells' exposure time to PAW and applying
342 higher PBR discharge frequencies. The highest reduction of the planktonic cells was observed

343 at 1500 Hz when the number of cells was below the detection level of 1.00 Log CFU ml⁻¹. Our
344 results agree with the study by Xiang et al. (2018), who reported that PAW produced by a
345 pressure plasma jet system (input power set at 750 W) effectively inactivated *P. deceptionensis*
346 CM2 planktonic cells in a time-dependent manner. Similarly, Tan and Karwe (2021) observed
347 the reduction of *Enterobacter aerogenes* planktonic cells floating in a pipe system after PAW
348 by approximately 3.50 Log CFU ml⁻¹. Inhibition of corrosive bacteria, e.g. *P. aeruginosa*, in
349 the water phase is a critical step in avoiding further colonization of industrial or medical
350 surfaces and interaction with other bacteria, fungi and viruses that can cause severe infections
351 in humans (Smith et al. 2015; Hendricks et al. 2016). It is important to highlight that the ability
352 of *P. aeruginosa* to grow and co-exist with other microorganisms in communal biofilms has
353 been associated with increased resistance against antimicrobials and disinfection strategies
354 (Pinto et al. 2020; del Mar Cendra and Torrents, 2021). Usually, the origin of bacterial
355 inactivation is linked to the formation of specific molecules during PAW generation (e.g.,
356 H₂O₂, nitrate and nitrite). However, it has also been shown that the transient electric fields
357 linked to the generation of cold plasma/plasma activated liquids can induce membrane
358 permeabilization, which can also contribute to cell damage and death (Naidis, 2010; Zhang, et
359 al. 2014; Robert et al. 2015; Chung et al. 2020; Vijayarangan et al. 2020; Dozias et al. 2021).
360 The inactivation depends on several factors such as bacterial species (gram-positive or negative
361 strains), physiological state of the microorganism (exponential or stationary growth), the
362 growth medium and the mode of growth (planktonic or biofilm) (Smet et al. 2019; Mai-
363 Prochnow et al. 2021a).

364 To investigate the mechanism of the antimicrobial effect of PAW on *P. aeruginosa*, the
365 intracellular ATP levels were monitored. ATP is required for many essential cellular functions
366 such as growth, replication, and survival (Shi et al. 2016). PAW treatment significantly reduced
367 the intercellular ATP levels of planktonic *P. aeruginosa* cells, and this ATP reduction increased

368 with PBR discharge frequencies. These results are consistent with Qian et al. (2021)
369 observations, who showed that cold plasma treatment decreased the ATP levels of *L.*
370 *monocytogenes* and *S. Enteritidis* cells. The reduction of intracellular ATP in *P. aeruginosa*
371 observed in our study could be attributed to an increase in the cell membrane permeability and
372 the resulting ATP leakage (Bajpai et al. 2013). Also, our study demonstrated that PAW
373 treatment resulted in protein leakage from the cells, suggesting a gradual increase in the
374 bacterial cell membrane permeability with an increase in PBR discharge frequency. This might
375 be due to the damage of the membrane by the increasing levels of the reactive species produced
376 in PAW.

377 Application of PAW as a treatment against the biofilms of gram-negative and gram-positive
378 bacteria is an emerging field of study (Chen et al. 2017; Kaushik et al. 2018). Our study also
379 investigated the effect of PAW on the more resistant biofilms of *P. aeruginosa*. The most
380 effective PBR discharge frequency of (1500 Hz) was used against different maturity biofilms
381 levels grown on SS surfaces. Numerous studies have previously described the mechanism of
382 biofilm formation by *P. aeruginosa* (Morales et al. 1993; Klausen et al. 2003; Yuan et al. 2007;
383 Harmsen et al. 2010) and their strong ability to further oxidize the substrate, thus leading to
384 severe pitting corrosion (Yuan et al. 2008; Hamzah et al. 2013). It is known that *P. aeruginosa*
385 biofilms can lead to microbial corrosion of different steel types such as SS 316 and 304
386 (Hamzah et al. 2013; Gabriel et al. 2016), C1018 (Jia et al. 2017), and other metallic surfaces
387 (Beech and Sunner, 2004; Wang et al. 2004; González et al. 2019). This study showed that
388 PAW treatment significantly reduces the level of bacterial cells and that this reduction
389 depended on the maturity of the biofilms. Patange et al. (2021) demonstrated inactivation of
390 early and mature *Escherichia coli* and *Listeria innocua* biofilm cells by atmospheric air plasma
391 (AAP). They showed that a 5 min AAP treatment reduced the cell count by approximately 3.5
392 to 4.5 Log CFU ml⁻¹. Gabriel et al. (2016) reported a 5-Log reduction of *P. aeruginosa* biofilm

393 cells on SS type 304 and 316 with different surface finishes after treatment with atmospheric
394 plasma for 90 s. Castro et al. (2021) investigated the removal of *P. fluorescens* and *P.*
395 *aeruginosa* biofilm cells; they used peracetic acid, sodium hypochlorite and Chlorhexidine
396 digluconate at concentrations recommended by the manufacturers and observed a much lower
397 than 5-Log cycles reduction. As a general observation, chlorine disinfection requires a
398 relatively longer time to reach a similar Log reduction compared to PAW treatment. This can
399 be attributed to chlorine's lower ability to disrupt the biofilm cells' exopolysaccharide (EPS)
400 matrix (Myszka and Czaczyk, 2011). Therefore, these findings demonstrate a strong potential
401 of PAW treatment against microorganisms that can cause microbial corrosion in the absence
402 of carcinogenic and mutagenic chlorine compounds (Meireles et al. 2016; Thorman et al.
403 2018).

404 PAW is considered a promising technology, showing apparent suitability to substitute more
405 traditional treatments used in a wide range of sectors, e.g. chlorine-based (Xiang et al. 2018;
406 Pantage et al. 2021). However, as PAW is yet a novel technology, a detailed investigation of
407 its mechanism of action and potential interactions with EPS matrix and other biofilm
408 compounds is yet to be performed. It is well known that biofilm maturity significantly affects
409 plasma penetration because thicker biofilms with more biomass provide a better protection
410 against reactive species (Chen et al. 2017; Hathaway et al. 2019; Patange et al. 2021). The same
411 effect was observed in the current study, when the 72 h mature biofilms were found to be most
412 resistant against PAW treatment. The presence of a complex mix of many reactive species in
413 PAW has been described as a significant antimicrobial factor affecting matrix degradation
414 (Tian et al. 2015; Cherny et al. 2020; Mai-Prochnow et al. 2021a). When the matrix is
415 disrupted, it is observed that biofilm cells can detach as either individual cells or larger cell
416 clusters, thus leaving small gaps in the biofilm structure (Mai-Prochnow et al. 2004). This
417 proposed mechanism of PAW interaction with biofilms relies on the reactive species to disrupt

418 the EPS matrix and release the sessile cells that can change their physiological state back to a
419 more susceptible planktonic state. Furthermore, Li et al. (2019) have shown that biofilm
420 treatment with PAW can downregulate the virulence genes linked to quorum sensing,
421 presenting an opportunity for the disruption and removal of biofilm cells.

422 The nature and amount of reactive species produced in PAW vary depending on the methods
423 used to generate them, which affects the PAW efficacy in various applications (Chen et al.
424 2018; Thirumdas et al. 2018; Zhou et al. 2020). PAW efficacy will also be influenced by
425 storage time and conditions (Zhao et al. 2020), which should be taken into since there could be
426 a delay between PAW generation and application. Plasma represents a highly reactive
427 environment, and in the case of PAW, the main reactive species present are hydroxyl radicals
428 ($\text{OH}\bullet$), hydrogen peroxide (H_2O_2), ozone (O_3), superoxide (O_2^-), nitric oxide ($\text{NO}\bullet$) and
429 peroxynitrite (ONOOH) all with a crucial role in bacterial inactivation (Han et al. 2016; Mai-
430 Prochnow et al. 2021a). However, some short-lived reactive species present, such as hydroxyl
431 radicals ($\text{OH}\bullet$), singlet oxygen ($^1\text{O}_2$), and superoxide (O_2^-) also have shown to contribute to
432 microbial inactivation although to a lesser extent (Surowsky et al. 2016; Liao et al. 2018).

433 Hydrogen peroxide (H_2O_2) monitored in the current study is one of the most common long-
434 lived reactive species found in PAW, which, together with nitrite (NO_2^-) and nitrate (NO_3^-),
435 play a significant role in microbial inactivation and biofilm removal (Park et al. 2017). In the
436 current study, nitrate followed by nitrite anions showed the highest concentrations among the
437 reactive species identified, illustrating the potential high efficacy of the PAW treatment against
438 *P. aeruginosa* planktonic cells and biofilms at 1500 Hz for 15 min. This is consistent with data
439 from other studies reporting that long-lived NO_2^- , NO_3^- , and H_2O_2 reactive species are efficient
440 against a wide range of bacteria, that can contaminate different types of surfaces (Naïtali et al.
441 2010; Shen et al. 2016; Xiang et al. 2018; Zhao et al. 2020). Mai-Prochnow et al. (2021b)
442 recently proved that a higher PBR discharge frequency leads to a higher production of reactive

443 species. The present study demonstrated that the higher level of reactive species generated with
444 the highest PAW treatment frequency leads to increased bacterial inactivation.

445 The higher EC observed in the current study provided further evidence for the accumulation of
446 the reactive species in PAW, leading to high inactivation of both planktonic cells and biofilms
447 of *P. aeruginosa*. The plasma treatment resulted in a significant drop in the pH of PAW,
448 however, the final pH was not low enough to be considered as a contributing factor to
449 antimicrobial activity. The extent of the pH drop observed, can be explained by the fact that
450 tap water was used to produce PAW and that its initial pH was approximately 7.56. Also, it
451 could possibly be attributed to H⁺ reacting with the different components in PAW and thus
452 result in a less pronounced pH drop. Bacteria inactivation mechanism in liquids is a result of
453 complex interactions at the plasma/gas–liquid-interface. The same applied for the subsequent
454 reactions in the liquid volume, and these interactions have not yet been fully described
455 (Oehmigen et al. 2011; Xiang et al. 2018).

456 Application of modelling can be beneficial for developing MIC mitigating strategies. As far as
457 inactivation of microorganisms in water systems is concerned, dynamic modelling has been
458 recently used to evaluate the thermal inactivation of *L. pneumophila* in water and proved an
459 efficient preventive approach for plumbing systems (Papagianeli et al. 2021). In the current
460 study, the log linear model developed confirmed our experimental results showing that PAW
461 treatment at 1500 Hz is the most effective with a Dt value of 2.24 comparing with 8.53 at 500
462 Hz against the planktonic cells of *P. aeruginosa*. Apparently, such trend may be associated
463 with the reactive species produced at PAW at different PBR discharge frequencies. The mature
464 (48 h and 72 h) biofilms were the most resistant, while according to the weighted least square
465 linear fit model (R²), the models had a good fit to the experimental data. Several factors affect
466 biofilm removal, and little is known about the relationship between the level of maturity and
467 the treatment exposure. Our results can provide valuable data on the inhibition of the planktonic

468 cells of *P. aeruginosa* that can colonise the metallic surfaces creating corrosive biofilms or
469 even removing the most resistant biofilms with PAW treatment.

470 This work has highlighted the efficiency of the PAW treatment against planktonic cells and
471 biofilms of *P. aeruginosa* grown on stainless-steel coupons. Reduction of intracellular ATP
472 levels and increase in protein release in of *P. aeruginosa* cells was attributed to an increased
473 membrane permeability due to the effect of reactive species in PAW. The 72 h mature biofilms
474 were found to be most resistant against PAW treatment compared to younger biofilms. The
475 observed reduction in the number of bacterial cells indicate the potential of the PAW as a means
476 for reduction of *P. aeruginosa* planktonic cells as well as biofilms grown on stainless-steel
477 contact surfaces. Results of this research demonstrate that this novel methodology can be
478 effectively used as an environmentally friendly method to inhibit MIC. A potential way to
479 apply this technology in a practical way to inhibit MIC would be by flushing existing pipe
480 systems with PAW or by generating PAW inside the pipe system. However, if the former
481 application method is used then the stability of the PAW between production and application
482 will have to be determined. Future work will focus on assessing the efficacy of PAW treatment
483 against other microorganisms causing corrosion in specific applications such as fire
484 engineering sprinkler maintenance, and pipe system maintenance in the food and medical
485 industries that contribute to MIC.

486 **ACKNOWLEDGEMENTS**

487 This work was supported by the University of West of England -Bristol internal funding
488 awarded to Alexandros Ch. Stratakos.

489 **CONFLICT OF INTEREST**

490 The authors declare no conflict of interest.

491 **AUTHOR CONTRIBUTIONS**

492

493 **Eleni Asimakopoulou:** Methodology, Software, Formal analysis, Data curation, Investigation,
494 Writing – original draft, Writing – review & editing. **Sotirios I. Ekonomou:** Methodology,
495 Formal analysis, Investigation, Data curation, Writing – original draft, Writing – review &
496 editing. **Pagona Papakonstantinou:** Investigation, Writing – review & editing. **Olena Doran:**
497 Methodology, Investigation, Writing – review & editing, Supervision. **Alexandros Ch.**
498 **Stratakos:** Conceptualization, Methodology, Investigation, Writing – review & editing,
499 Supervision, Funding acquisition.

500 **DATA AVAILABILITY STATEMENT**

501 The data that support the findings of this study are available from the corresponding author
502 upon reasonable request.

503

504 **REFERENCES**

- 505 Abdolahi, A., Hamzah, E., Ibrahim, Z. and Hashim, S. (2014). Microbially influenced
506 corrosion of steels by *Pseudomonas aeruginosa*. *Corrosion Reviews*, 32(3-4), pp.129-141.
- 507 Alshraiedeh, N. A. H., Kelly, S. A., Thompson, T. P., Flynn, P. B., Tunney, M. M., Gilmore,
508 B. F. (2020). Extracellular polymeric substance-mediated tolerance of *Pseudomonas*
509 *aeruginosa* biofilms to atmospheric pressure non-thermal plasma treatment. *Plasma Processes*
510 *and Polymers*, 17(12), 2000108.
- 511 Bajpai, V. K., Sharma, A., Baek, K. H. (2013). Antibacterial mode of action of *Cudrania*
512 *tricuspidata* fruit essential oil, affecting membrane permeability and surface characteristics of
513 food-borne pathogens. *Food control*, 32(2), 582-590.
- 514 Bardal, E., 2007. *Corrosion and protection*. Springer Science & Business Media.
- 515 Beech, I. B., Sunner, J. (2004). Biocorrosion: towards understanding interactions between
516 biofilms and metals. *Current opinion in Biotechnology*, 15(3), 181-186.

517 Ben Belgacem, Z., Carré, G., Charpentier, E., Le-Bras, F., Maho, T., Robert, E., Povesle,
518 J.M., Polidor, F., Gangloff, S.C., Boudifa, M. and Gelle, M.P. (2017). Innovative non-thermal
519 plasma disinfection process inside sealed bags: Assessment of bactericidal and sporicidal
520 effectiveness in regard to current sterilization norms. *PLoS One*, 12(6), e0180183.

521 Bigelow, W. D., Esty, J. R. (1920). The thermal death point in relation to time of thermophilic
522 microorganisms. *The Journal of Infectious Diseases*, 602-617.

523 Bourke, P., Ziuzina, D., Han, L., Cullen, P. J., & Gilmore, B. F. (2017). Microbiological
524 interactions with cold plasma. *Journal of applied microbiology*, 123(2), 308-324.

525 Castro, M. S. R., da Silva Fernandes, M., Kabuki, D. Y., Kuaye, A. Y. (2021). Modelling
526 *Pseudomonas fluorescens* and *Pseudomonas aeruginosa* biofilm formation on stainless steel
527 surfaces and controlling through sanitisers. *International Dairy Journal*, 114, 104945.

528 Chen, T.P., Liang, J. and Su, T.L. (2018). Plasma-activated water: antibacterial activity and
529 artifacts?. *Environmental Science and Pollution Research*, 25(27), pp.26699-26706.

530 Chen, T. P., Su, T. L., Liang, J. (2017). Plasma-activated solutions for bacteria and biofilm
531 inactivation. *Current Bioactive Compounds*, 13(1), 59-65.

532 Cheng, S., Tian, J., Chen, S., Lei, Y., Chang, X., Liu, T. and Yin, Y. (2009). Microbially
533 influenced corrosion of stainless steel by marine bacterium *Vibrio natriegens*:(I) Corrosion
534 behavior. *Materials Science and Engineering: C*, 29(3), pp.751-755.

535 Cherny, K. E., Sauer, K. (2020). Untethering and degradation of the polysaccharide matrix are
536 essential steps in the dispersion response of *Pseudomonas aeruginosa* biofilms. *Journal of*
537 *bacteriology*, 202(3).

538 Chung, T.H., Stancampiano, A., Sklias, K., Gazeli, K., André, F.M., Dozias, S., Douat, C.,
539 Povesle, J.M., Santos Sousa, J., Robert, E. and Mir, L.M. (2020). Cell electropermeabilisation
540 enhancement by non-thermal-plasma-treated pbs. *Cancers*, 12(1), 219

541 del Mar Cendra, M., Torrents, E. (2021). *Pseudomonas aeruginosa* biofilms and their partners
542 in crime. *Biotechnology Advances*, 107734.

543 Dozias, S., Pouvesle, J. M. and Robert, E., (2021). Comment on ‘Mapping the electric field
544 vector of guided ionization waves at atmospheric pressure’, (2020) *Plasma Res. Express* 2
545 025014. *Plasma Research Express*, 3(3), p.038001.

546 Ekonomou, S. I., Boziaris, I. S. (2021). Non-Thermal Methods for Ensuring the
547 Microbiological Quality and Safety of Seafood. *Applied Sciences*, 11(2), 833.

548 Ehlbeck, J., Schnabel, U., Polak, M., Winter, J., Von Woedtke, T., Brandenburg, R., Von dem
549 Hagen, T. and Weltmann, K.D. (2010). Low temperature atmospheric pressure plasma sources
550 for microbial decontamination. *Journal of Physics D: Applied Physics*, 44(1), 013002.

551 EPA (2006) Data Quality Assessment: Statistical Methods for Practitioners, U.S.
552 Environmental Protection Agency, EPA QA/G-9S.

553 Enning, D. and Garrelfs, J. (2014). Corrosion of iron by sulfate-reducing bacteria: new views
554 of an old problem. *Applied and environmental microbiology*, 80(4), pp.1226-1236.

555 Flemming H. C. (1996). Economical and technical overview. In: Heitz E, Flemming H-C, Sand
556 W, Microbially influenced corrosion of materials, New York: *Springer*, 5–14.

557 Gabriel, A. A., Ugay, M. C. C. F., Siringan, M. A. T., Rosario, L. M. D., Tumlos, R. B., Ramos,
558 H. J. (2016). Atmospheric pressure plasma jet inactivation of *Pseudomonas aeruginosa*
559 biofilms on stainless steel surfaces. *Innovative Food Science and Emerging Technologies*, 36,
560 311-319.

561 Geeraerd, A.H., Valdramidis, V. P., Van Impe, J. F. (2005). GIaFiT, a freeware tool to assess
562 non log-linear microbial survivor curves. *International Journal of Food Microbiology*, 102,
563 95-105.

564 Gonzalez-Gonzalez, C. R., Hindle, B. J., Saad, S., Stratakos, A. C. (2021). Inactivation of
565 *Listeria monocytogenes* and *Salmonella* on Stainless Steel by a Piezoelectric Cold
566 Atmospheric Plasma Generator. *Applied Sciences*, 11(8), 3567.

567 González, E.A., Leiva, N., Vejar, N., Sancy, M., Gulppi, M., Azócar, M.I., Gomez, G.,
568 Tamayo, L., Zhou, X., Thompson, G.E. and Páez, M.A. (2019). Sol-gel coatings doped with
569 encapsulated silver nanoparticles: inhibition of biocorrosion on 2024-T3 aluminum alloy
570 promoted by *Pseudomonas aeruginosa*. *Journal of Materials Research and Technology*, 8(2),
571 pp.1809-1818.

572 Hamzah, E., Hussain, M. Z., Ibrahim, Z., Abdolahi, A. (2013). Influence of *Pseudomonas*
573 *aeruginosa* bacteria on corrosion resistance of 304 stainless steel. *Corrosion engineering,*
574 *science and technology*, 48(2), 116-120.

575 Han, L., Boehm, D., Patil, S., Cullen, P. J., Bourke, P. (2016). Assessing stress responses to
576 atmospheric cold plasma exposure using *Escherichia coli* knock-out mutants. *Journal of*
577 *applied microbiology*, 121(2), 352-363.

578 Harmsen, M., Yang, L., Pamp, S. J., Tolker-Nielsen, T. (2010). An update on *Pseudomonas*
579 *aeruginosa* biofilm formation, tolerance, and dispersal. *FEMS Immunology & Medical*
580 *Microbiology*, 59(3), 253-268.

581 Hathaway, H.J., Patenall, B.L., Thet, N.T., Sedgwick, A.C., Williams, G.T., Jenkins, A.T.A.,
582 Allinson, S.L. and Short, R.D. (2019). Delivery and quantification of hydrogen peroxide
583 generated via cold atmospheric pressure plasma through biological material. *Journal of Physics*
584 *D: Applied Physics*, 52(50), p.505203.

585 Hendricks, M.R., Lashua, L.P., Fischer, D.K., Flitter, B.A., Eichinger, K.M., Durbin, J.E.,
586 Sarkar, S.N., Coyne, C.B., Empey, K.M. and Bomberger, J.M. (2016). Respiratory syncytial
587 virus infection enhances *Pseudomonas aeruginosa* biofilm growth through dysregulation of

588 nutritional immunity. *Proceedings of the National Academy of Sciences*, 113(6), pp.1642-
589 1647.

590 Herrera L. K., Videla H. A. (2009). Role of iron-reducing bacteria in corrosion and protection
591 of carbon steel. *International Biodeterioration and Biodegradation*, 63, 891 – 895
592 (<https://doi.org/10.1016/j.ibiod.2009.06.003>).

593 Ibrahim A., Hawboldt K., Bottaro C., Khan F. (2018). Review and analysis of
594 microbiologically influenced corrosion: the chemical environment in oil and gas facilities,
595 *Corrosion Engineering, Science and Technology*, 53(8), 549-563
596 (<https://doi.org/10.1080/1478422X.2018.1511326>).

597 Jayathunge, K. G. L. R., Stratakos, A. C., Delgado-Pando, G., Koidis, A. (2019). Thermal and
598 non-thermal processing technologies on intrinsic and extrinsic quality factors of tomato
599 products: A review. *Journal of Food Processing and Preservation*, 43(3), e13901.

600 Jia, R., Yang, D., Xu, J., Xu, D., & Gu, T. (2017). Microbiologically influenced corrosion of
601 C1018 carbon steel by nitrate reducing *Pseudomonas aeruginosa* biofilm under organic carbon
602 starvation. *Corrosion Science*, 127, 1-9.

603 Jia, R., Yang, D., Xu, D., & Gu, T. (2017). Anaerobic corrosion of 304 stainless steel caused
604 by the *Pseudomonas aeruginosa* biofilm. *Frontiers in microbiology*, 8, 2335.

605 Julák, J., Scholtz, V., Kotúčová, S., & Janoušková, O. (2012). The persistent microbicidal
606 effect in water exposed to the corona discharge. *Physica Medica*, 28(3), 230-239.

607 Katsigiannis, A. S., Bayliss, D. L., & Walsh, J. L. (2021). Cold plasma decontamination of
608 stainless steel food processing surfaces assessed using an industrial disinfection protocol. *Food*
609 *Control*, 121, 107543.

610 Kaushik, N. K., Ghimire, B., Li, Y., Adhikari, M., Veerana, M., Kaushik, N., ... & Choi, E. H.
611 (2018). Biological and medical applications of plasma-activated media, water and solutions.
612 *Biological chemistry*, 400(1), 39-62.

613 Kermani B., Harrop D. (2019). Corrosion and materials in hydrocarbon production: a
614 compendium of operational and engineering aspects, *John Wiley, and Sons*.

615 Klausen, M., Heydorn, A., Ragas, P., Lambertsen, L., Aaes-Jørgensen, A., Molin, S., Tolker-
616 Nielsen, T. (2003). Biofilm formation by *Pseudomonas aeruginosa* wild type, flagella and type
617 IV pili mutants. *Molecular microbiology*, 48(6), 1511-1524.

618 Koch G., Varmey J., Thompson N., Moghissi O., Gould M., Payer J. (2016). International
619 measures of prevention, application, and economics of corrosion technologies study, Gretchen
620 Jacobson, *NACE International*, Houston, Texas, USA.

621 Levine, A. D., Harwood, V. J., Fox, G. A. (2009). Collecting, Exploring, and Interpreting
622 Microbiological Data Associated with Reclaimed Water Systems. *Water Environment*
623 *Research Foundation*: Alexandria, VA, USA.

624 Li, Y., Pan, J., Wu, D., Tian, Y., Zhang, J., Fang, J. (2019). Regulation of *Enterococcus faecalis*
625 biofilm formation and quorum sensing related virulence factors with ultra-low dose reactive
626 species produced by plasma activated water. *Plasma Chemistry and Plasma Processing*, 39(1),
627 35-49.

628 Li H., Zhou E., Zhang D., Xu D., Xia J., Yang C., Feng H., Jiang Z., Li X., Gu T., Yang K.
629 (2016). Microbiologically Influenced Corrosion of 2707 Hyper-Duplex Stainless Steel by
630 Marine *Pseudomonas aeruginosa* Biofilm. *Scientific Reports*, 6, 20190.

631 Liao, X., Su, Y., Liu, D., Chen, S., Hu, Y., Ye, X., Wang, J. and Ding, T. (2018). Application
632 of atmospheric cold plasma-activated water (PAW) ice for preservation of shrimps
633 (*Metapenaeus ensis*). *Food Control*, 94, pp.307-314.

634 Line, L., Alhede, M., Kolpen, M., Kühl, M., Ciofu, O., Bjarnsholt, T., Moser, C., Toyofuku,
635 M., Nomura, N., Høiby, N. and Jensen, P.Ø. (2014). Physiological levels of nitrate support
636 anoxic growth by denitrification of *Pseudomonas aeruginosa* at growth rates reported in cystic
637 fibrosis lungs and sputum. *Frontiers in microbiology*, 5, 554.

638 Little, B.J., Blackwood, D.J., Hinks, J., Lauro, F.M., Marsili, E., Okamoto, A., Rice, S.A.,
639 Wade, S.A. and Flemming, H.C. (2020). Microbially influenced corrosion—any
640 progress?. *Corrosion Science*, 170, 108641.

641 Ma, R., Wang, G., Tian, Y., Wang, K., Zhang, J., Fang, J. (2015). Non-thermal plasma-
642 activated water inactivation of food-borne pathogen on fresh produce. *Journal of hazardous*
643 *materials*, 300, 643-651.

644 Mai-Prochnow, A., Zhou, R., Zhang, T., Ostrikov, K. K., Mugunthan, S., Rice, S. A., Cullen,
645 P. J. (2021a). Interactions of plasma-activated water with biofilms: inactivation, dispersal
646 effects and mechanisms of action. *NPJ biofilms and microbiomes*, 7(1), 1-12.

647 Mai-Prochnow, A., Alam, D., Zhou, R., Zhang, T., Ostrikov, K., Cullen, P. J. (2021b).
648 Microbial decontamination of chicken using atmospheric plasma bubbles. *Plasma Processes*
649 *and Polymers*, 18(1), 2000052.

650 Mai-Prochnow, A., Evans, F., Dalisay-Saludes, D., Stelzer, S., Egan, S., James, S., Webb, J.S.
651 and Kjelleberg, S. (2004). Biofilm development and cell death in the marine bacterium
652 *Pseudoalteromonas tunicata*. *Applied and environmental microbiology*, 70(6), pp.3232-3238.

653 Maxwell, S. (2006). Predicting Microbiologically Influenced Corrosion (MIC) in seawater
654 systems. *2006 SPE International Oil Field Corrosion Symposium*, Aberdeen, UK: Society of
655 Petroleum Engineers.

656 Meireles, A., Giaouris, E., Simões, M. (2016). Alternative disinfection methods to chlorine for
657 use in the fresh-cut industry. *Food Research International*, 82, 71-85.

658 Morales, J., Esparza, P., Gonzalez, S., Salvarezza, R. Arevalo, M. P. (1993). The role of
659 *Pseudomonas aeruginosa* on the localised corrosion of 304 stainless steel. *Corrosion science*,
660 34(9), 1531-1540.

661 Myszka, K., Czaczyk, K. (2011). Bacterial biofilms on food contact surfaces-a review. *Polish*
662 *Journal of Food and Nutrition Sciences*, 61(3).

663 Naidis, G.V. (2010). Modelling of streamer propagation in atmospheric-pressure helium
664 plasma jets. *Journal of Physics D: Applied Physics*, 43(40), p.402001.

665 Naïtali, M., Kamgang-Youbi, G., Herry, J. M., Bellon-Fontaine, M. N., & Brisset, J. L. (2010).
666 Combined effects of long-living chemical species during microbial inactivation using
667 atmospheric plasma-treated water. *Applied and environmental microbiology*, 76(22), 7662-
668 7664.

669 Oehmigen, K., Winter, J., Hähnel, M., Wilke, C., Brandenburg, R., Weltmann, K. D., & von
670 Woedtke, T. (2011). Estimation of possible mechanisms of *Escherichia coli* inactivation by
671 plasma treated sodium chloride solution. *Plasma Processes and Polymers*, 8(10), 904-913.

672 Ogden, T. L. (2010). Handling results below the level of detection. *The Annals of occupational*
673 *hygiene*, 54(3), 255-256.

674 Pan, J., Li, Y.L., Liu, C.M., Tian, Y., Yu, S., Wang, K.L., Zhang, J. and Fang, J. (2017).
675 Investigation of cold atmospheric plasma-activated water for the dental unit waterline system
676 contamination and safety evaluation in vitro. *Plasma Chemistry and Plasma Processing*, 37(4),
677 pp.1091-1103.

678 Papagianeli, S. D., Aspidou, Z., Didos, S., Chochlakis, D., Psaroulaki, A., & Koutsoumanis,
679 K. (2021). Dynamic modelling of *Legionella pneumophila* thermal inactivation in water. *Water*
680 *Research*, 190, 116743.

681 Park, J. Y., Park, S., Choe, W., Yong, H. I., Jo, C., Kim, K. (2017). Plasma-functionalized
682 solution: A potent antimicrobial agent for biomedical applications from antibacterial
683 therapeutics to biomaterial surface engineering. *ACS applied materials and interfaces*, 9(50),
684 43470-43477.

685 Patange, A. D., Simpson, J. C., Curtin, J. F., Burgess, C. M., Cullen, P. J., & Tiwari, B. K.
686 (2021). Inactivation efficacy of atmospheric air plasma and airborne acoustic ultrasound
687 against bacterial biofilms. *Scientific Reports*, 11(1), 1-14.

688 Pasquali, F., Stratakos, A.C., Koidis, A., Berardinelli, A., Cevoli, C., Ragni, L., Mancusi, R.,
689 Manfreda, G. and Trevisani, M. (2016). Atmospheric cold plasma process for vegetable leaf
690 decontamination: A feasibility study on radicchio (red chicory, *Cichorium intybus* L.). *Food*
691 *control*, 60, pp.552-559.

692 Phan, H. C., Blackall, L. L., & Wade, S. A. (2021). Effect of Multispecies Microbial Consortia
693 on Microbially Influenced Corrosion of Carbon Steel. *Corrosion and Materials*
694 *Degradation*, 2(2), 133-149.

695 Pinto, R. M., Soares, F. A., Reis, S., Nunes, C., Van Dijck, P. (2020). Innovative strategies
696 toward the disassembly of the EPS matrix in bacterial biofilms. *Frontiers in Microbiology*, 11.

697 Qian, J., Ma, L., Yan, W., Zhuang, H., Huang, M., Zhang, J. and Wang, J. (2021). Inactivation
698 kinetics and cell envelope damages of foodborne pathogens *Listeria monocytogenes* and
699 *Salmonella Enteritidis* treated with cold plasma. *Food Microbiology*, p.103891.

700 Robert, E., Darny, T., Dozias, S., Iseni, S. and Pouvesle, J.M. (2015). New insights on the
701 propagation of pulsed atmospheric plasma streams: From single jet to multi jet arrays. *Physics*
702 *of plasmas*, 22(12), p.122007.

703 Sadiq, M. B., Tarning, J., Aye Cho, T. Z., Anal, A. K. (2017). Antibacterial activities and
704 possible modes of action of *Acacia nilotica* (L.) Del. against multidrug-resistant *Escherichia*
705 *coli* and *Salmonella*. *Molecules*, 22(1), 47.

706 Shen, J., Tian, Y., Li, Y., Ma, R., Zhang, Q., Zhang, J., and Fang, J. (2016). Bactericidal effects
707 against *S. aureus* and physicochemical properties of plasma activated water stored at different
708 temperatures. *Scientific reports*, 6(1), 1-10.

709 Silvestri, E.E., Yund, C., Taft, S., Bowling, C.Y., Chappie, D., Garrahan, K., Brady-Roberts,
710 E., Stone, H., and Nichols, T.L. (2017). Considerations for estimating microbial environmental
711 data concentrations collected from a field setting. *Journal of Exposure Science and*
712 *Environmental epidemiology*, 27(2), 141-151.

713 Skovhus, T. L., Taylor, C., Eckert, R. B. (2019). Modeling of Microbiologically influenced
714 corrosion – Limitations and perspectives. *CRC press*.

715 Smet, C., Govaert, M., Kyrylenko, A., Easdani, M., Walsh, J. L., Van Impe, J. F. (2019).
716 Inactivation of single strains of *Listeria monocytogenes* and *Salmonella typhimurium*
717 planktonic cells biofilms with plasma activated liquids. *Frontiers in microbiology*, *10*, 1539.

718 Smith, K., Rajendran, R., Kerr, S., Lappin, D. F., Mackay, W. G., Williams, C., & Ramage, G.
719 (2015). *Aspergillus fumigatus* enhances elastase production in *Pseudomonas aeruginosa* co-
720 cultures. *Medical mycology*, *53*(7), 645-655.

721 Stratakos, A.C., Sima, F., Ward, P., Linton, M., Kelly, C., Pinkerton, L., Stef, L., Pet, I. and
722 Corcionivoschi, N. (2018). The in vitro effect of carvacrol, a food additive, on the pathogenicity
723 of O157 and non-O157 Shiga-toxin producing *Escherichia coli*. *Food Control*, *84*, pp.290-296.

724 Su P., Fuller D.B. (2014). Corrosion and corrosion mitigation in fire protection systems,
725 *Research Technical Report FM Global*.

726 Surowsky, B., Bußler, S., & Schlüter, O. K. (2016). Cold plasma interactions with food
727 constituents in liquid and solid food matrices. In *Cold plasma in food and agriculture* (pp. 179-
728 203). Academic Press.

729 Tan, J., Karwe, M. V. (2021). Inactivation and removal of *Enterobacter aerogenes* biofilm in a
730 model piping system using plasma-activated water (PAW). *Innovative Food Science &*
731 *Emerging Technologies*, *69*, 102664.

732 Thirumdas, R., Kothakota, A., Annapure, U., Siliveru, K., Blundell, R., Gatt, R., &
733 Valdramidis, V. P. (2018). Plasma activated water (PAW): Chemistry, physico-chemical
734 properties, applications in food and agriculture. *Trends in food science & technology*, *77*, 21-
735 31.

736 Thorman, R.E., Nicholson, F.A., Topp, C.F., Bell, M.J., Cardenas, L.M., Chadwick, D.R.,
737 Cloy, J.M., Misselbrook, T.H., Rees, R.M., Watson, C.J. and Williams, J.R. (2020). Towards

738 country-specific nitrous oxide emission factors for manures applied to arable and grassland
739 soils in the UK. *Frontiers in Sustainable Food Systems*, 4, p.62.

740 Tian, Y., Ma, R., Zhang, Q., Feng, H., Liang, Y., Zhang, J. and Fang, J., 2015. Assessment of
741 the physicochemical properties and biological effects of water activated by non-thermal plasma
742 above and beneath the water surface. *Plasma processes and polymers*, 12(5), pp.439-449.

743 Wang, W., Wang, J., Li, X., Xu, H., Wu, J. (2004). Influence of biofilms growth on corrosion
744 potential of metals immersed in seawater. *Materials Corrosion–Werkstoffe Korrosion*, 55, 30-
745 35.

746 Vijayarangan, V., Delalande, A., Dozias, S., Pouvesle, J.M., Robert, E. and Pichon, C. (2020).
747 New insights on molecular internalization and drug delivery following plasma jet exposures.
748 *International Journal of Pharmaceutics*, 589, p.119874.

749 Xiang, Q., Kang, C., Niu, L., Zhao, D., Li, K., & Bai, Y. (2018). Antibacterial activity and a
750 membrane damage mechanism of plasma-activated water against *Pseudomonas deceptionensis*
751 CM2. *LWT*, 96, 395-401.

752 Xu, D., Xia, J., Zhou, E., Zhang, D., Li, H., Yang, C., Li, Q., Lin, H., Li, X. and Yang, K.
753 (2017). Accelerated corrosion of 2205 duplex stainless steel caused by marine aerobic
754 *Pseudomonas aeruginosa* biofilm. *Bioelectrochemistry*, 113, pp.1-8.

755 Xu, D., Li, Y., & Gu, T. (2016). Mechanistic modeling of biocorrosion caused by biofilms of
756 sulfate reducing bacteria and acid producing bacteria. *Bioelectrochemistry*, 110, 52-58.

757 Yuan, S. J., Pehkonen, S. O., Ting, Y. P., Kang, E. T., Neoh, K. G. (2008). Corrosion behavior
758 of type 304 stainless steel in a simulated seawater-based medium in the presence and absence
759 of aerobic *Pseudomonas NCIMB 2021* bacteria. *Industrial and engineering chemistry*
760 *research*, 47(9), 3008-3020.

761 Yuan, S. J., Choong, A. M., Pehkonen, S. O. (2007). The influence of the marine aerobic
762 Pseudomonas strain on the corrosion of 70/30 Cu–Ni alloy. *Corrosion science*, 49(12), 4352-
763 4385.

764 Zhao, Y.M., Ojha, S., Burgess, C.M., Sun, D.W. and Tiwari, B.K. (2020). Inactivation efficacy
765 and mechanisms of plasma activated water on bacteria in planktonic state. *Journal of applied*
766 *microbiology*, 129(5), pp.1248-1260.

767 Zhang, Q., Zhuang, J., von Woedtke, T., Kolb, J.F., Zhang, J., Fang, J. and Weltmann, K.D.
768 (2014). Synergistic antibacterial effects of treatments with low temperature plasma jet and
769 pulsed electric fields. *Applied Physics Letters*, 105(10), p.104103.

770 Zhou, R., Zhou, R., Wang, P., Xian, Y., Mai-Prochnow, A., Lu, X., Cullen, P.J., Ostrikov, K.K.
771 and Bazaka, K. (2020). Plasma-activated water: generation, origin of reactive species and
772 biological applications. *Journal of Physics D: Applied Physics*, 53(30), p.303001.

773 Zhou, R., Zhou, R., Prasad, K., Fang, Z., Speight, R., Bazaka, K., Ostrikov, K. K. (2018). Cold
774 atmospheric plasma activated water as a prospective disinfectant: the crucial role of
775 peroxy nitrite. *Green Chemistry*, 20(23), 5276-5284.

776 **FIGURE LEGENDS**

777 **FIGURE 1.** Schematic representation of the PBR used to generate the PAW consisting of an
778 acrylic tube submerged into water, high-voltage power supply to generate atmospheric plasma
779 under atmospheric conditions and supply of compressed air at a flow rate of 1 L/min.

780 **FIGURE 2.** Reduction of *P. aeruginosa* planktonic cells after 5, 10, and 15 min of exposure
781 to PAW at PBR discharge frequencies of 500, 1000, and 1500 Hz. Each bar represents the
782 mean value of three replicates, each of which was analyzed twice. The error bars represent the
783 Standard Deviation for Mean (n = 6). The values with uppercase letters followed by the same
784 lowercase letters did not differ significantly between the exposure times ($P > 0.05$). The values
785 with uppercase letters followed by different lowercase letters differed significantly between
786 exposure times ($P < 0.05$). Asterisk (*) indicates the values which were below the detection
787 limit (1.00 Log CFU ml⁻¹)

788 **FIGURE 3.** Reduction of *P. aeruginosa* biofilms of different maturity (24, 48, and 72 h) after
789 5, 10, 15, and 20 min of exposure during PAW treatment at 1500 Hz. Each bar represents the
790 mean value of three replicates, each of which was analyzed twice. The error bars represent the
791 Standard Deviation for Mean (n = 6). The values with uppercase letters followed by the same
792 lowercase letters did not differ significantly between the exposure times ($P > 0.05$). The values
793 with uppercase letters followed by different lowercase letters differed significantly between
794 exposure times ($P < 0.05$). Asterisk (*) indicates the values which were below the detection
795 limit (2.00 Log CFU cm²-1)

796 **FIGURE 4.** Release of proteins from *P. aeruginosa* Control (untreated cells) and from cells
797 treated with PAW at PBR discharge frequencies of 500, 1000, and 1500 Hz. The error bars
798 represent the Standard Deviation for Mean (n = 3). The treatments with different lowercase
799 letters differ significantly ($P < 0.05$)

800 **FIGURE 5.** Intracellular ATP production by *P. aeruginosa* untreated (Control) and by the cells
 801 treated with PAW at different PBR discharge frequencies. The error bars represent the Standard
 802 Deviation for Mean (n = 3). The treatments with different lowercase letters differ significantly
 803 ($P < 0.05$)

804 **FIGURE 6.** Inactivation curves of *P. aeruginosa* biofilms of different maturity under the
 805 treatment with 1500 Hz frequency. Censored data were handled using a substitution method,
 806 using half the detection limit. Each point represents the mean value of six replicates

807 **FIGURE 7.** Inactivation curves of *P. aeruginosa* planktonic cells after 5, 10, and 15 min of
 808 exposure during PAW treatment at PBR discharge frequencies of 500, 1000, and 1500 Hz.
 809 Censored data were handled using a substitution method, using half the detection limit. Each
 810 point represents the mean value of six replicates

811
 812 **TABLE 1.** Physicochemical parameters and reactive molecular species in PAW after 15 min
 813 exposure at 1500 Hz

Treatments	pH	EC (mS cm ⁻¹)	H ₂ O ₂ (mg ml ⁻¹)	NO ₂ ⁻ (mg ml ⁻¹)	NO ₃ ⁻ (mg ml ⁻¹)
Tap water*	7.56±0.02 ^A	230.667±2.73 ^A	-	-	-
PAW	5.94±0.04 ^B	325.333±11.64 ^B	0.03±0.002	0.04± 0.001	0.04±0.001

814 *Tap water prior to the use of PBR to generate PAW.

815 The results are presented as mean ± standard deviation (SD). The mean values were calculated
 816 for three replicates, each of which was analyzed twice (n=6).

817 Values in the same column with different uppercase letters differ significantly ($P < 0.05$).

818

819

820 **TABLE 2.** Model parameters and associated errors for biofilm cells of different maturity (24,
 821 48, and 72 h) after 5, 10 and 15 of exposure to PAW treatment at 1500 Hz

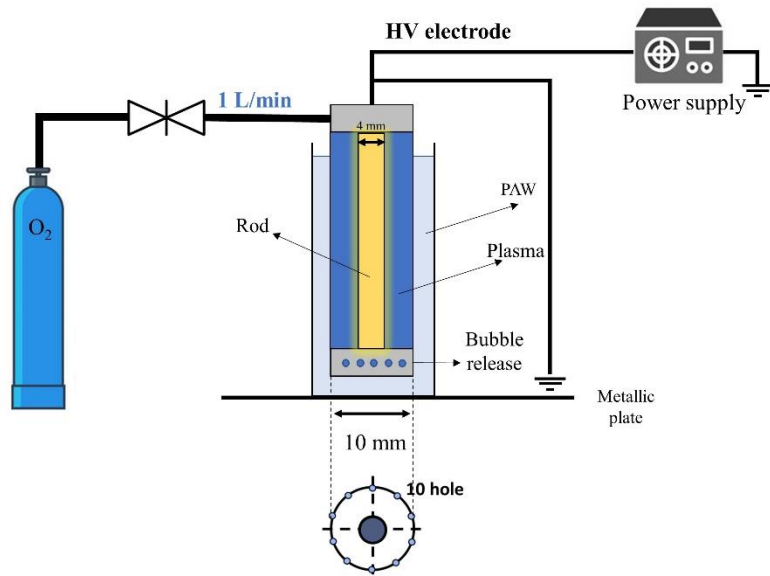
Biofilm maturity (h)	Parameters							
	D_T	SE	$\log N_o$	SE	Mean Sum of R^2	R^2 Root Mean Sum	R^2	R^2 adjusted
24	3.11	0.13	5.51	0.53	0.3965	0.6296	0.9417	0.9125
48	4.34	0.09	5.67	0.46	0.3507	0.5922	0.9253	0.9005
72	4.19	0.07	6.21	0.36	0.2102	0.4585	0.9548	0.9445

822
 823 **TABLE 3.** Model parameters and associated errors of *P. aeruginosa* planktonic cells after 5,
 824 10, and 15 min of exposure during PAW treatment at PBR discharge frequencies of 500,
 825 1000, and 1500 Hz

PBR discharge frequencies (Hz)	Parameters							
	D_T	SE	$\log N_o$	SE	Mean Sum of R^2	R^2 Root Mean Sum	R^2	R^2 adjusted
500	8.53	0.02	5.03	0.10	0.0147	0.1213	0.9833	0.9749
1000	3.44	0.04	4.89	0.16	0.0374	0.1933	0.9930	0.9895
1500	2.24	0.07	4.90	0.20	0.0479	0.2188	0.9953	0.9906

826
 827
 828
 829
 830
 831
 832
 833

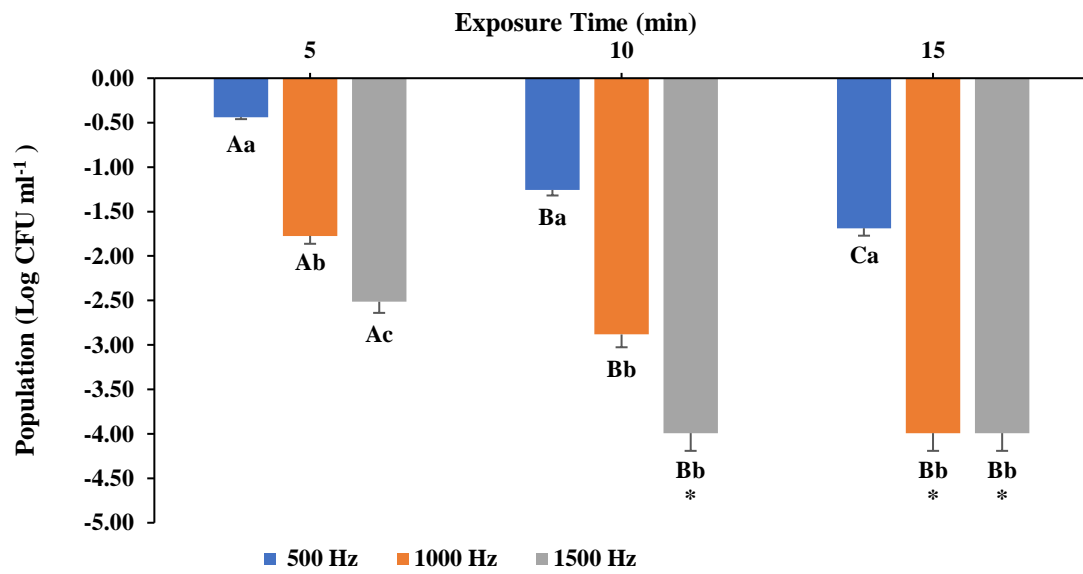
834 **FIG 1**



835

1

836 **FIG 2**



837

838

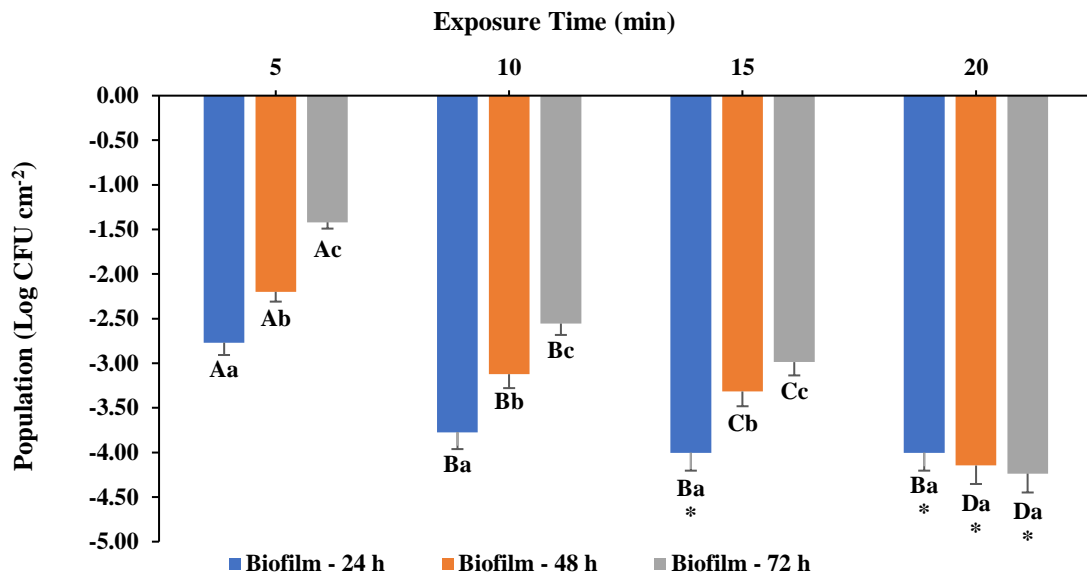
839

840

841

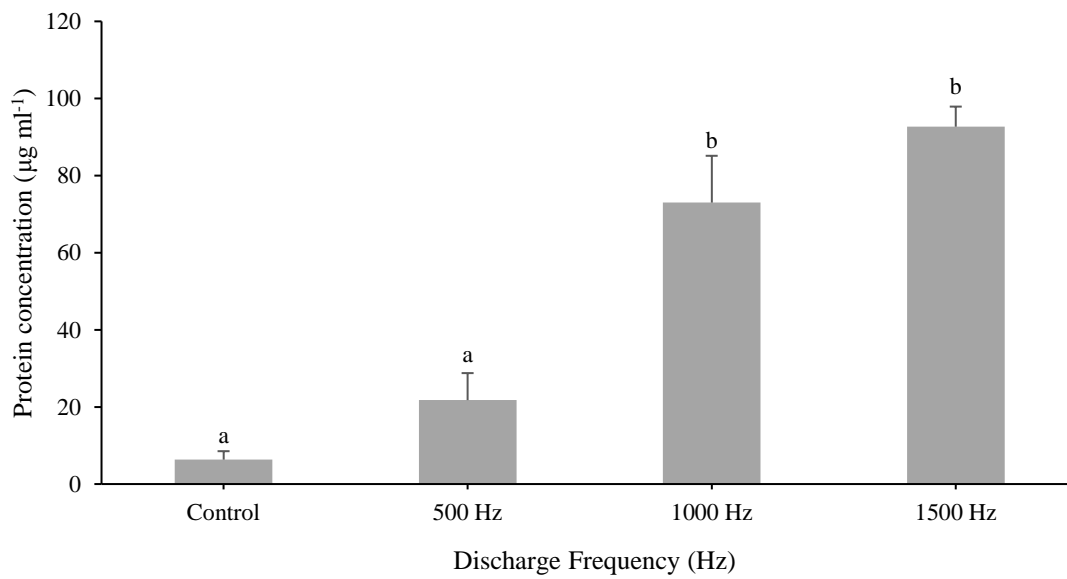
842

843 **FIG 3**



844

845 **FIG 4**



846

847

848

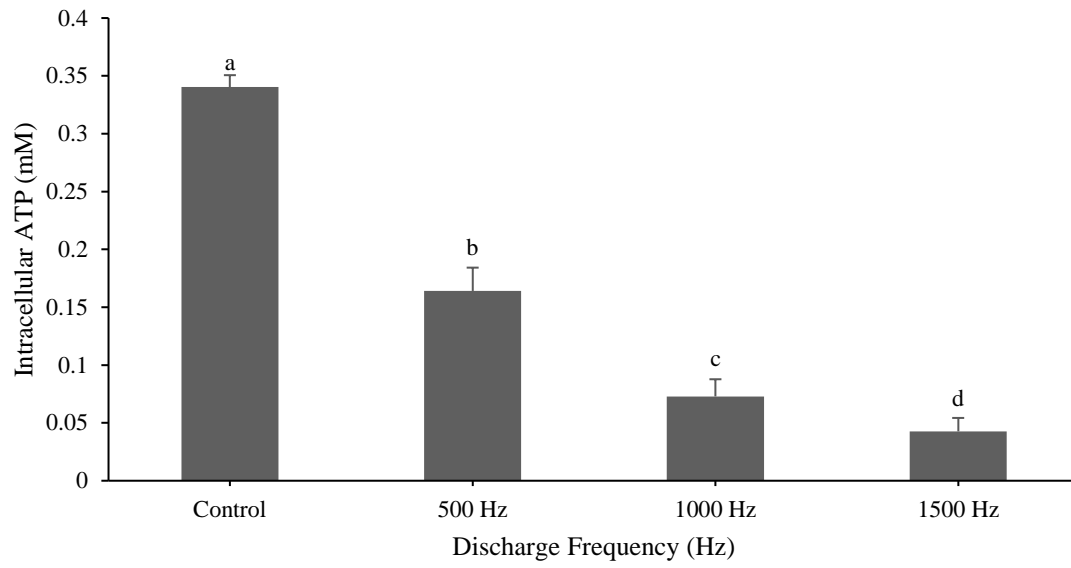
849

850

851

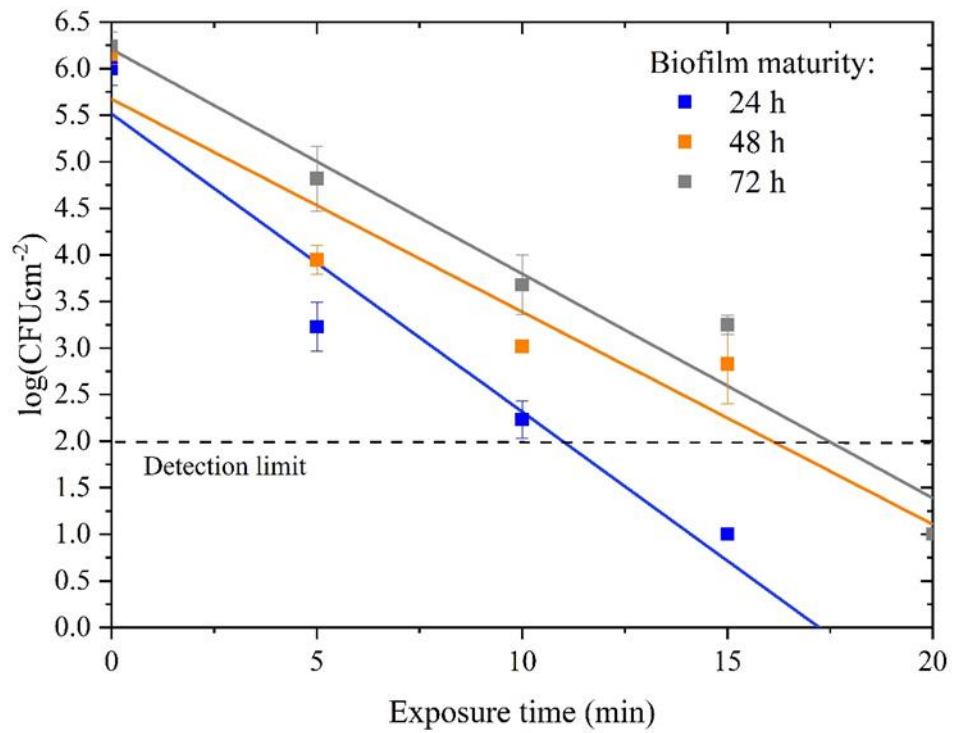
852

853 **FIG 5**



854

855 **FIG 6**

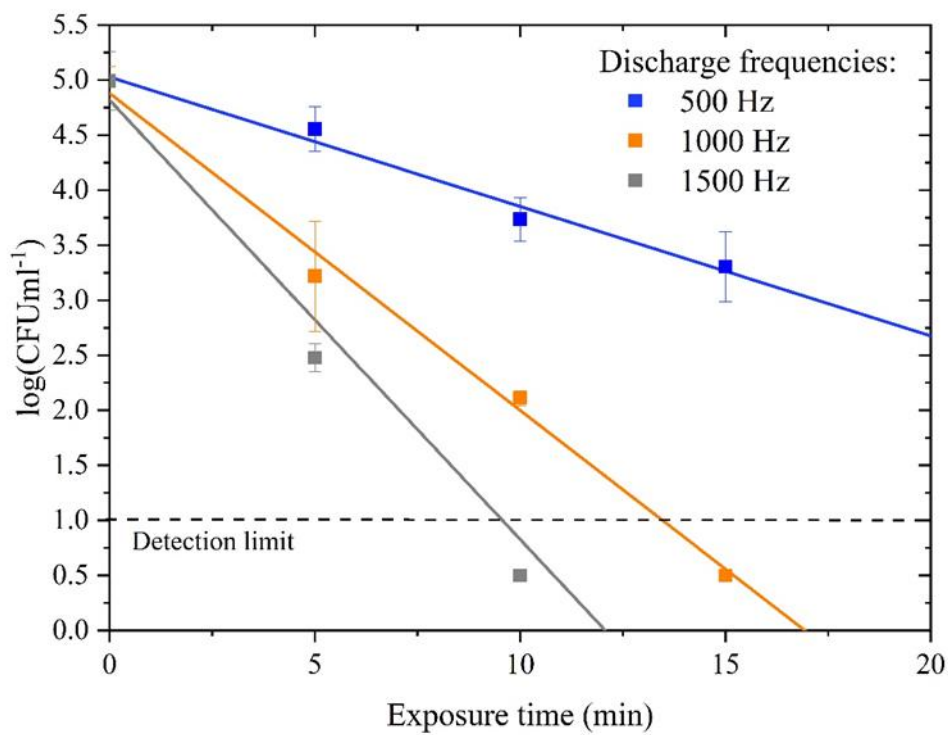


856

857

858

859



861

862

863

864